IEEE Access
Multidisciplinary | Rapid Review | Open Access Journal

Date of publication xxxx 00, 0000, date of current version xxxx 00, 0000.

Digital Object Identifier 10.1109/ACCESS.2017.Doi Number

Design of a Single-Radiator Multi-Port Compact Chip Antenna for UWB Direction-Finding

HYUNMU KANG[1], SANGWOON YOUN[2], AND HOSUNG CHOO[1] (Senior Member, IEEE)

[1]Department of Electronic and Electrical Engineering, Hongik University, Seoul 04066, South Korea
[2]Department of Digital Information and Communication Technology Engineering, Gyeongkuk National University, Andong 36729, South Korea

Corresponding author: Sangwoon Youn (e-mail: syoun@gknu.ac.kr)

This work was supported by the Samsung Research Funding Center of Samsung Electronics under Project SRFC-IT1801-51.

ABSTRACT This paper proposes a single-radiator multi-port (SRMP) compact chip antenna for ultra-wideband (UWB) direction-finding. The antenna proposed in this paper is miniaturized to a physical size of 11.5 mm × 9.46 mm × 1.6 mm by utilizing a ceramic substrate with high-permittivity of 20. Furthermore, we designed a CPW feed line for the proposed chip antenna and verified its performance when mounted on a board through simulation and measurement. This small structure includes a multi-port system that can replace a conventional array system, utilizing the tripod-shaped single radiator. To verify the feasibility, the proposed antenna is fabricated and the antenna characteristics such as reflection coefficients, mutual couplings, and radiation patterns are measured in a full anechoic chamber. The proposed antenna has an operating bandwidth of 7 GHz to 9 GHz, which makes it well-suited for UWB Channel 9 (7.737 GHz – 8.236 GHz) in Korean mobile devices. The measured mutual coupling result is below −10 dB across the operating frequency band. In addition, the radiation patterns in the *zx*-plane and *zy*-plane are anlayzed, and a bore-sight gain of 4.2 dBi is observed at 8 GHz. To verify the direction-finding performance, the proposed antenna is connected to the Nordic board nRF52840 DK with the commercial Qorvo DW3000 module to obtain channel impulse response (CIR) data. Then, the direction of arrival (DoA) is measured at distances of 0.3 m, 1 m, and 2 m according to the incident angle from −30° to 30°. The root mean square (RMS) errors at distances are 1.1°, 1.2°, and 1.5°, respectively. These results demonstrate that the proposed compact chip antenna is suitable for use in mobile devices equipped with UWB direction-finding technology.

INDEX TERMS UWB direction-finding, single-radiator multi-port, chip antenna

I. INTRODUCTION

Ultra-wideband (UWB) technology has attracted significant attention in modern wireless communication systems due to its advantages such as wide frequency band, low power consumption, and immunity to multipath interference [1], [2], [3], [4]. In particular, UWB technology provides high-resolution location data because it has a narrow pulse width due to the wide bandwidth of more than 500 MHz. Therefore, this technology is utilized in various direction-finding applications for high-accuracy indoor positioning services. As technological advances lead to significantly smaller devices, research on miniaturizing UWB antennas is actively being conducted. Previous studies have proposed various design techniques to miniaturize UWB antennas, but several limitations remain. Studies [5], [6], [7], [8] achieved wideband characteristics using a single monopole structure. However, when implemented in array configurations, it is difficult to maintain sufficient spacing between elements and requires large mounting areas. Also, research [9], [10], [11], [12] introduced slot structures in the radiator to enhance bandwidth, but there is still a problem that the antenna size is too large to be mounted into compact mobile device. Studies on chip antennas [13], [14], [15], [16] employed high-permittivity ceramic substrates combined with spiral or slot structures for miniaturization. Nevertheless, these designs lack multi-port configurations required for direction-finding, limiting their ability to replace traditional array systems. To address these challenges, studies have proposed multi-port UWB antennas. However, they often suffer from degraded wideband performance [17], [18], [19], [20] or large array dimensions unsuitable for mobile platforms [21], [22], [23], [24]. More recent works [25], [26], [27], [28] introduced single radiator multi-port (SRMP) designs in which multiple ports share a common radiator. While this approach reduces complexity, the resulting antenna size is still impractical for devices like smartphones, smart tags, or

smartwatches. Moreover, these studies do not sufficiently consider PCB integration or realistic mounting conditions within actual devices. To realize practical UWB direction-finding systems for smartphone applications, the following three requirements must be addressed. First, an array system capable of performing direction-finding is essential for UWB localization systems. Second, miniaturization of conventional UWB systems is necessary to enable the integration of UWB technology into compact mobile devices such as smartwatches and smart tags, and smartphones. Finally, a design approach that considers PCB board mounting is required to minimize the need for additional mounting structures.

In this paper, we propose a single-radiator multi-port (SRMP) compact chip antenna for UWB direction-finding. The proposed antenna adopts a tripod-shaped SRMP structure to reduce the size of the array system while achieving broadband characteristics of UWB channel 9. The antenna is optimized for UWB Channel 9 (7.737–8.236 GHz) in accordance with frequency regulations for mobile UWB communications in South Korea, as specified in the IEEE 802.15.4a standard. The proposed tripod-shaped radiator with three ports is designed to replace conventional UWB array antennas, which typically require multiple physically separated radiating elements to achieve direction-finding capability. To further miniaturize the antenna size and minimize losses in the 7 GHz to 9 GHz frequency range, a high-permittivity ceramic substrate structure is employed. Additionally, to consider the condition of the antenna being mounted on the device with PCB, a main board with a coplanar waveguide (CPW) feed line is designed, and a very small MHF-7S connector is used for excitation. Through this process, the proposed antenna is designed, and its performance is analyzed considering the on-board environment using FEKO EM simulator [29]. To verify the feasibility, the proposed antenna is fabricated and the antenna characteristics such as reflection coefficients, mutual couplings, and radiation patterns are measured in a full anechoic chamber. Also, to better understand the operating principles of the proposed antenna, matching characteristics are investigated using key design parameters. In addition, the reflection coefficients and size of the proposed antenna are compared with those of miniaturized monopole antenna studies. Finally, to verify the direction-finding performance considering on-board environment, the transmit antenna is connected to the Nordic board nRF52840 DK with the commercial Qorvo DW3000 module. The proposed antenna is connected to the DW3000 module to obtain channel impulse response (CIR) data as receiver. Then, the estimated direction of arrival (DoA) result is measured according to the incident angle from −30° to 30°. These results demonstrate that the proposed antenna is suitable for use in mobile devices equipped with UWB direction-finding technology.

II. GEOMETRY AND PERFORMANCE OF THE PROPOSED ANTENNA

A. GEOMETRY OF THE PROPOSED ANTENNA

Fig. 1 shows the geometry of the proposed antenna, which consists of the chip antenna and the main board with three CPW feed lines. As shown in Fig. 1(a), the proposed antenna uses a single tripod-shaped radiator with widths of w_m and w_t and a length of l_t to achieve broadband characteristics while reducing the size of the array system. As Equation (1), w_m, w_t, and l_t represent the widths and length of a single tripod-shaped radiator, as illustrated in Fig. 1(a).

$$y = -2\left(\frac{\frac{w_t}{3}\sqrt{3}+l_t}{w_m - w_t}\right)\times\left(x+\frac{w_t}{2}\right)+\frac{w_t}{6}\sqrt{3},\ \ z = t+h \quad , \tag{1}$$

For further miniaturization, a high-permittivity ceramic substrate (ε_{rc} = 20, tanδ = 0.00028) with a length of l_c and height of h is employed, and the tripod-shaped radiator is printed on the substrate. Also, to obtain a wide bandwidth, the ceramic substrate is designed with a gap of g from the edge of the tripod-shaped radiator. Fig. 1(b) shows the proposed antenna mounted on the main board which is designed to consider integration with the PCB inside the mobile device. The main board uses an FR-4 substrate (ε_{rb} = 4.3, tanδ = 0.018) with a thickness of t. Three CPW feed lines on the main board are designed as $w_m \times l_m$ (width × length) for impedance matching on UWB channel 9. These feed lines are connected to a single tripod-shaped radiator at equal angular differences of ϕ_p to replace the array system for direction-finding. To enable direction-finding across all horizontal and vertical directions, at least three antennas are generally required. In order to implement this capability within a compact design, we configure three ports on a single tripod-shaped radiator. Then, the tripod-shaped radiator is connected to the three feed lines, respectively. In addition, mobile devices have limited mounting space, very small connectors are required for power supply. Thus, we utilize a compact MHF-7S connector with dimensions of 2 mm × 2 mm × 0.53 mm (width × length × height) to consider practical mounting conditions. Detailed design parameters are listed in Table 1. To determine the optimized values listed in Table 1, a parametric study for each design value is conducted to identify the configuration that maximizes impedance bandwidth while reducing coupling. The final values are chosen based on the combination that provides the best trade-off between broadband performance and compact size. By adjusting geometric parameters and substrate properties, the same design concept can be applied to operate at other UWB channels, including the broader 3.1 GHz to 10.6 GHz range defined by the Federal Communications Commission (FCC).

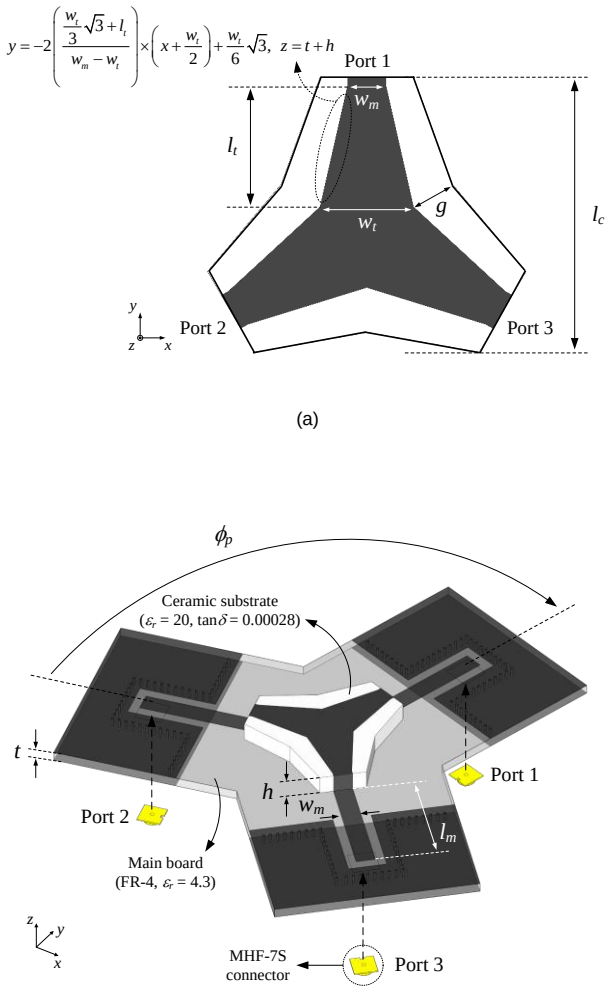

FIGURE 1. Geometry of the proposed antenna mounted on the main board. (a) Top view of the chip antenna. (b) Isometric view.

TABLE 1. Design parameters of the proposed antenna.

Parameters	Symbol	Optimized values
CPW feed line length	l_m	9.46 mm
Ceramic substrate length	l_c	11.5 mm
Radiator length	l_t	5 mm
Radiator width	w_t	4 mm
CPW feed line width	w_m	1.6 mm
Main board thickness (FR-4)	t	0.8 mm
Ceramic substrate height	h	1.6 mm
Angular differences between ports	ϕ_p	120°
Ceramic substrate permittivity	ε_{rc}	20
Main board permittivity (FR-4)	ε_{rb}	4.3
Gap between radiator and substrate	g	2 mm

B. FABRICATION AND MEASUREMENT

Fig. 2(a) shows a photograph of the fabricated UWB SRMP chip antenna. The single tripod-shaped radiator is etched onto a high-permittivity ceramic substrate and is soldered along three CPW feed lines on the main board, which is designed for mounting on the PCB in a mobile device. Then, each of the three input ports is fed from the bottom of the main board using a compact MHF-7S connector, generally used in mobile device PCBs, as shown in Fig. 2(b). To verify the feasibility, the fabricated antenna is measured in a full anechoic chamber to confirm the antenna performance such as the reflection coefficients, mutual coupling, and radiation patterns. Fig. 3 presents a comparison of the reflection coefficients for port 1 and mutual couplings between ports 1 and 2 of the proposed antenna. The measured and simulated reflection coefficients for port 1 are represented by solid and dashed lines, respectively, while the mutual coupling between ports 1 and 2 are indicated by dotted and dash-dotted lines, respectively. The measured reflection coefficient shows a broadband characteristic of less than −10 dB from 7 GHz to 9 GHz, showing a similar tendency to the simulation results. The proposed antenna shows the measured and simulated mutual couplings less than −12 dB across the entire operating frequency range, which satisfies typical isolation characteristics for single-radiator multi-port designs [30], [31], [32]. Fig. 4 presents the measured and simulated (using FEKO EM simulator) radiation patterns of the proposed antenna for port 1. Fig. 4(a) shows the measured (solid line) and simulated (dashed line) radiation pattern of the proposed antenna for port 1 in the *zx*-plane. The measured and simulated radiation patterns in the *zy*-plane are also shown in Fig. 4(b). The proposed antenna has measured and simulated bore-sight gains of 4.2 dBi and 4.3 dBi at 8 GHz, respectively. The asymmetry in the measured patterns is attributed to practical measurement factors. These include fabrication tolerances, loss introduced by the small MHF-7S connector, the influence of the coaxial cable connected to the connector, and slight misalignment of the antenna in the anechoic chamber during measurements. To verify that the proposed antenna operates over the entire UWB Channel 9 (from 7.6 GHz to 8.4 GHz), we observe the co- and cross-polarization patterns of the proposed antenna for port 1 at 7.6 GHz, 8 GHz, and 8.4 GHz. Fig. 5(a) shows the co-polarization (solid line) and cross-polarization (dashed line) patterns obtained by simulation for port 1 at 7.6 GHz. The patterns at 8 GHz and 8.4 GHz are also shown in Fig. 5(b) and (c). The co-pol. patterns have bore-sight gains of 1.8 dBi, 4.3 dBi, and 6 dBi at 7.6 GHz, 8 GHz, and 8.4 GHz, respectively. Fig. 6 shows the measured ('×' markers) and simulated (dashed line) bore-sight gains for port 1, indicating that the two results have similar tendency with frequency. Fig. 7 illustrates the measured and simulated radiation efficiencies. The measurement exhibits a radiation efficiency of 80.6% at 8 GHz, which is similar to the simulation result of 80.3%.

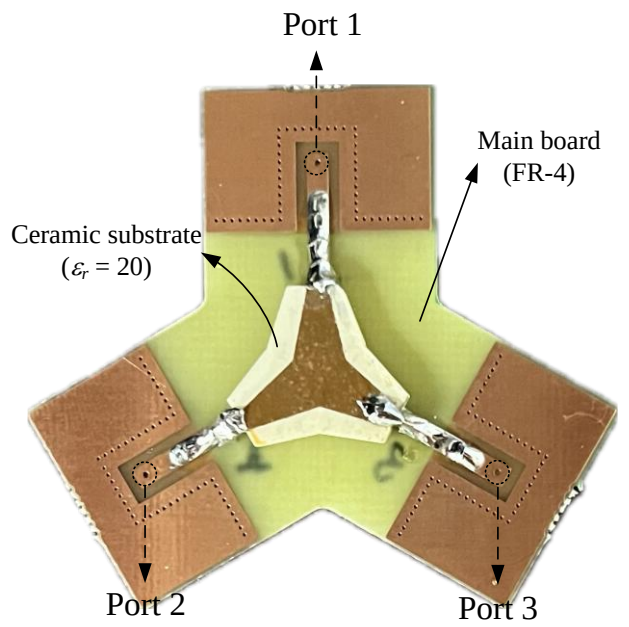

(a)

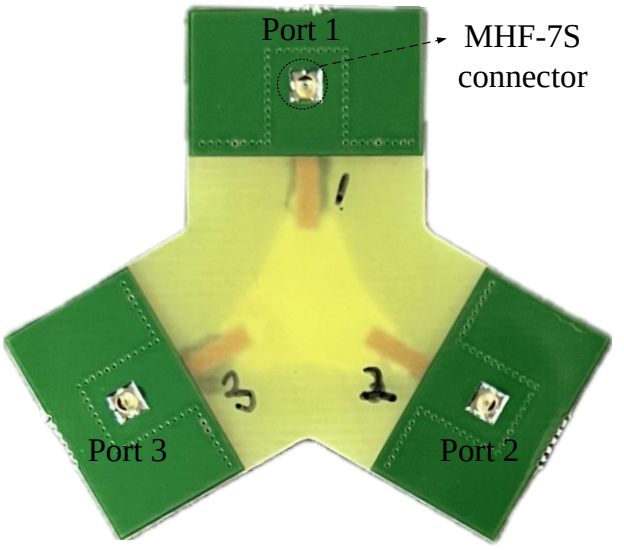

(b)

FIGURE 2. Photographs of the fabricated UWB SRMP chip antenna. (a) Top view. (b) Bottom view.

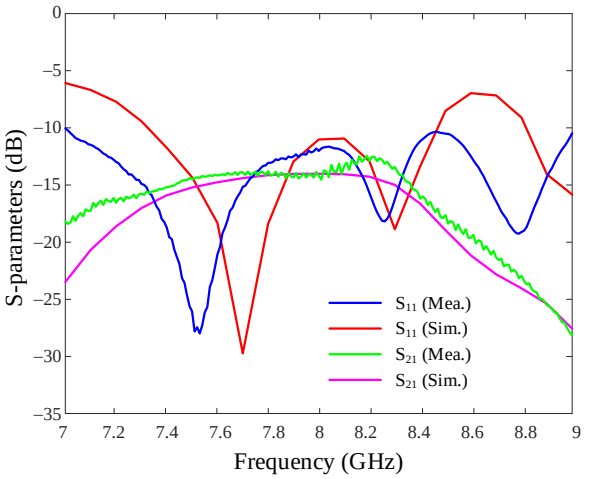

FIGURE 3. Measured and simulated reflection coefficients and mutual couplings of the proposed antenna.

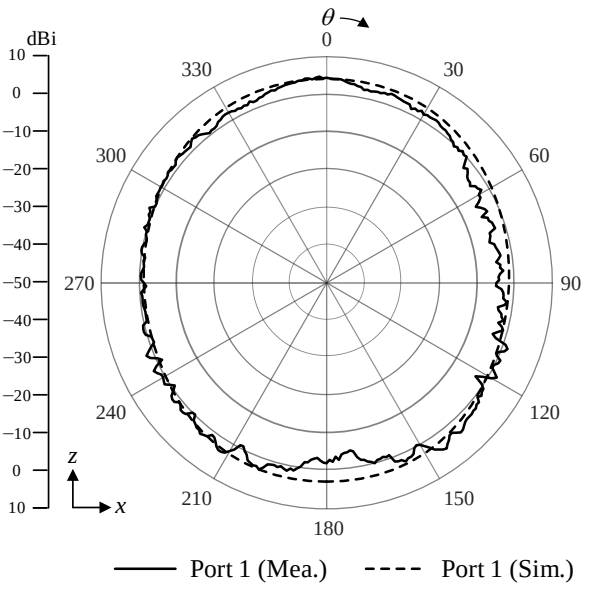

(a)

This article has been accepted for publication in IEEE Access. This is the author's version which has not been fully edited and content may change prior to final publication. Citation information: DOI 10.1109/ACCESS.2026.3662058

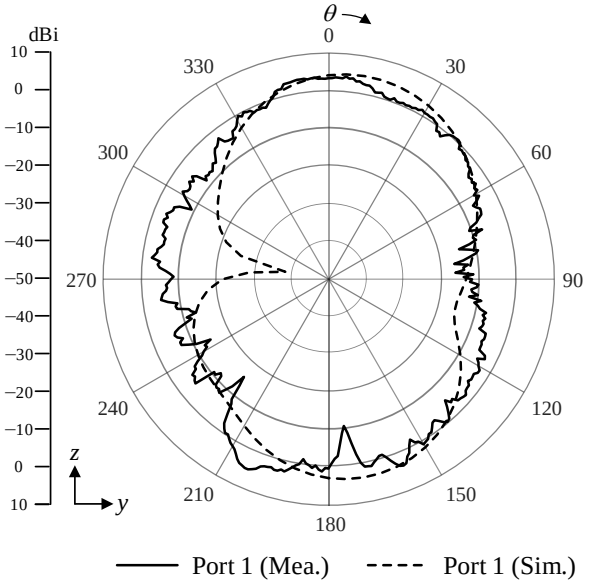

(b)

FIGURE 4. **Measured and simulated radiation patterns of the proposed antenna for port 1. (a) *zx*-plane. (b) *zy*-plane.**

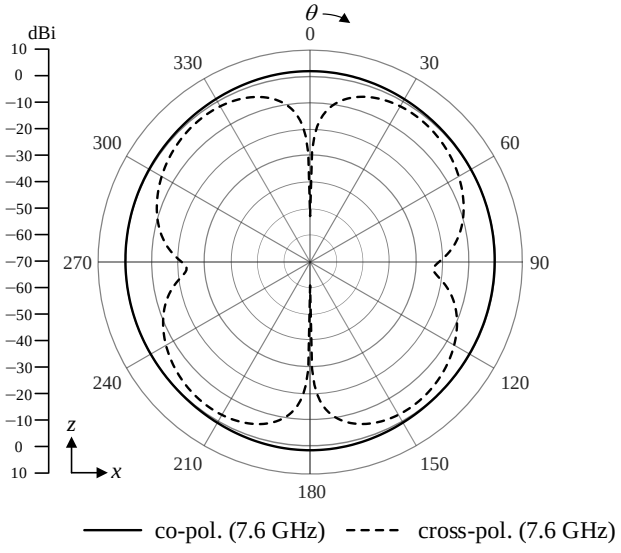

(a)

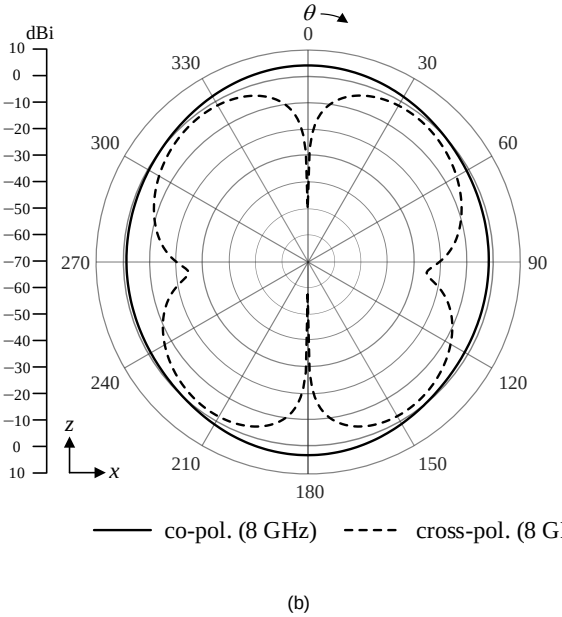

(b)

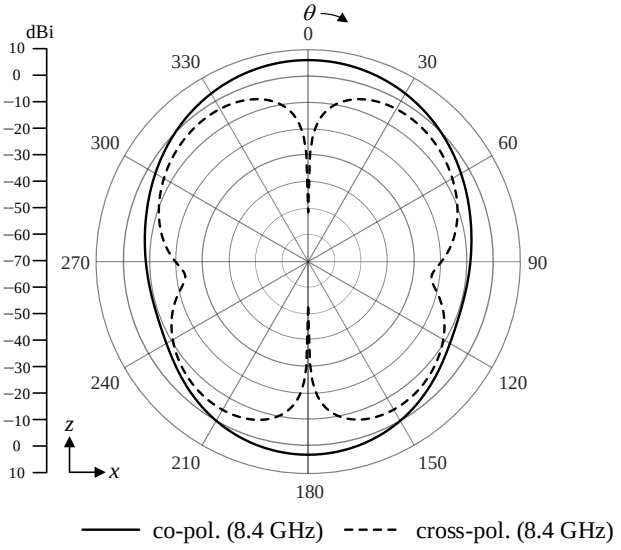

(c)

FIGURE 5. **Co- and cross- polarization patterns of the proposed antenna for port 1. (a) at 7.6 GHz. (b) at 8 GHz. (c) at 8.4 GHz**

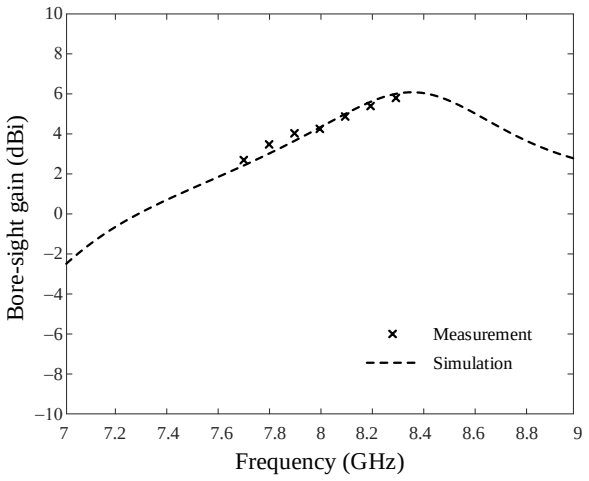

FIGURE 6. Measured and simulated bore-sight gains of the proposed antenna.

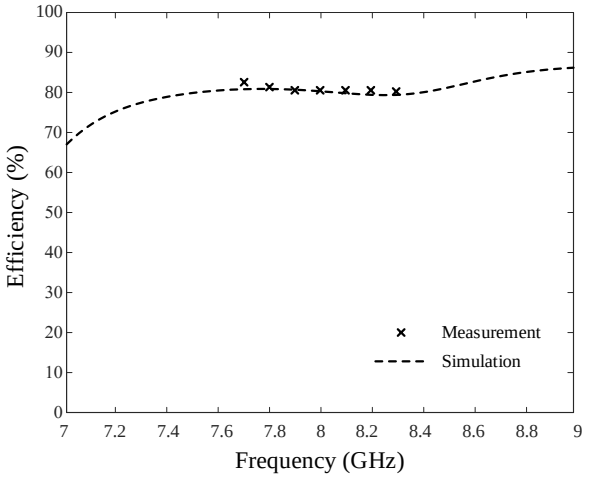

FIGURE 7. Comparison of the simulated and measured radiation efficiencies for port 1.

C. ANALYSIS OF THE DESIGN PARAMETERS

To conduct an in-depth analysis of the broadband characteristics of the proposed antenna, we investigate the key design parameters w_t, l_c, and g. Herein, w_t indicates the width of the center of the tripod-shaped radiating element, and l_c is the length of the ceramic substrate. Fig. 8(a) compares the reflection coefficients according to w_t. w_t varies from 2.8 mm to 5.2 mm, and a wide bandwidth of 1.1 GHz at the center frequency of 8 GHz is achieved when an optimal width $\underline{w_t}$ is 4 mm. To achieve broadband characteristics within a limited mounting space, parametric studies on the design parameters l_c and g of the ceramic substrate are conducted, as shown in Fig. 8(b) and 8(c). We analyze the reflection coefficients by varying the length l_c of the ceramic substrate (from 10.9 mm to 12.1 mm) and the gap g between the substrate and the edge of the radiator (from 0 mm to 4 mm). As a result, the proposed antenna has optimal broadband characteristics from 7.4 GHz to 8.5 GHz within a limited mounting space, when l_c is 11.5 mm and g is 2 mm. Furthermore, we analyze the impact of the ceramic substrate and tripod-shaped radiator on broadband performance and miniaturization by studying three monopole antenna cases with and without these components. These results illustrate how individual key parameters affect antenna performance. Although the final design is obtained through multi-parameter optimization using Genetic Algorithm (GA), the parametric studies are included to provide intuitive insight into the impact of each structural change on impedance matching and bandwidth. As shown in Fig. 9(a), Case 1 is a conventional monopole antenna printed on an FR-4 board without a ceramic substrate. Case 2 is a printed monopole antenna that has the same tripod-shaped radiator as the proposed antenna without the ceramic substrate. The case is designed to operate at 8 GHz and the bandwidth variation with and without the tripod-shaped radiator is investigated and compared with the proposed antenna. For fairness in comparison, each structure is individually adjusted to operate near this frequency. Dimensions of Cases 1 and 2 are determined through parametric adjustments to evaluate the effect of the tripod structure (Case 2) and the high-permittivity substrate (the proposed design). To also analyze the size variation with and without the ceramic substrate, we define the effective aperture size of each case as l_1, l_2, and l_p, respectively. Fig. 9(b) demonstrates that the proposed antenna achieves better impedance matching across the target band (7 GHz to 9 GHz) compared to Cases 1 and 2. The improvement is particularly evident near 8 GHz, where the proposed structure maintains a reflection coefficient consistently below –10 dB. When the tripod structure is applied to the radiator as Case 2, the fractional bandwidth (at center frequency of 8 GHz) significantly improves from 2% to 10.6%, but the effective aperture size increases from l_1 = 34.9 mm to l_2 = 36.9 mm. To solve this aperture size problem, a high-permittivity ceramic substrate is used. In antenna design, employing a high-permittivity substrate decreases the required wavelength at the target frequency, leading to a reduction in antenna size [33]. Accordingly, the effective aperture size l_p of the proposed antenna achieves a reduction of 39.8% compared to l_2. Also, as the current path extends by the height h of the ceramic substrate, additional resonance occurs at a frequency lower than 8 GHz, leading to a 3.2% increase in bandwidth. These results demonstrate that the proposed antenna is suitable not only for mobile devices such as smartphones, but also for small wearable devices such as smartwatches using UWB channel 9. In addition, by adjusting the radiator dimensions and substrate parameters, the same design concept can be re-optimized for other UWB allocations, broadening the range of applications.

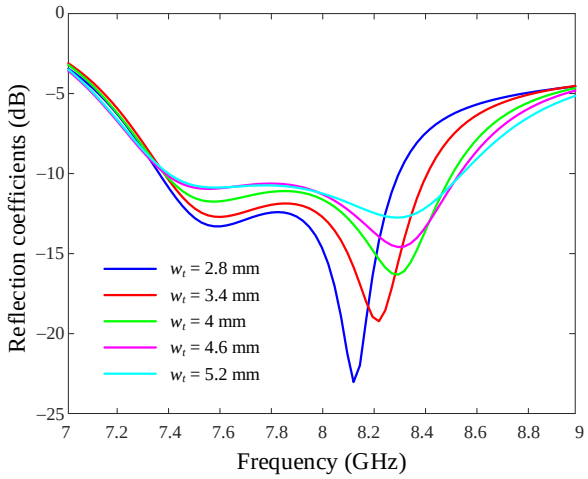

(a)

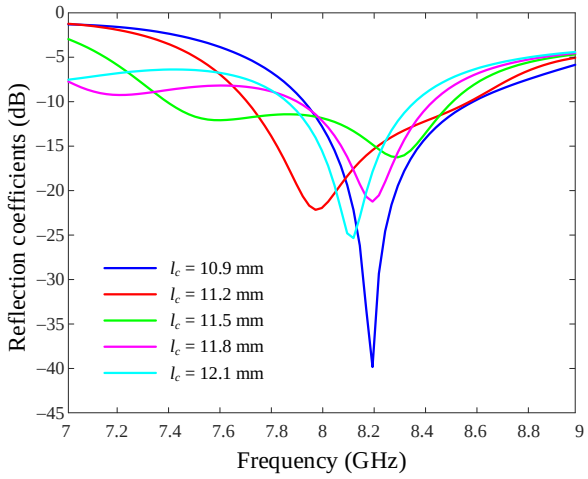

(b)

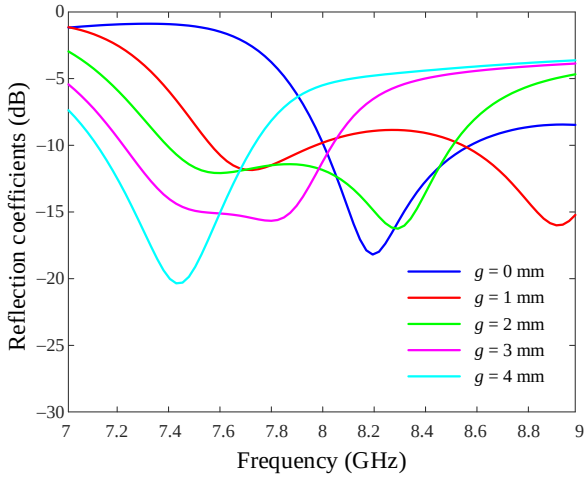

(c)

FIGURE 8. **Comparison of reflection coefficients depending on the width w_t, the length l_c, and the gap g. (a) Comparison of reflection coefficients depending on w_t. (b) Comparison of reflection coefficients depending on l_c. (c) Comparison of reflection coefficients depending on g.**

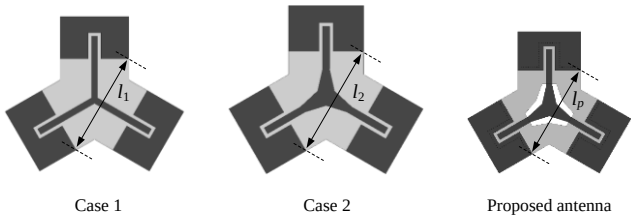

(a)

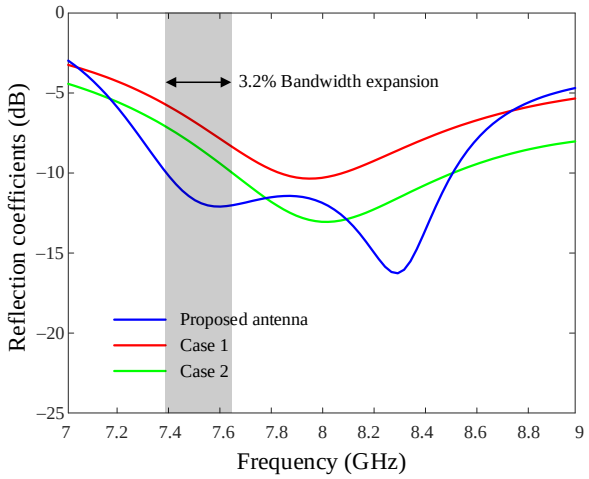

(b)

FIGURE 9. **Analysis of the miniaturization of the proposed antenna. (a) Investigated monopole antennas. (b) Reflection coefficients of the monopole antennas.**

III. DIRECTION OF ARRIVAL ESTIMATION USING CHANNEL IMPULSE RESPONSE DATA

To estimate the direction-finding performance of the proposed antenna, the measurement set-up is represented, as shown in Fig. 10. The transmitter is configured by connecting the commercial Qorvo DW3000 module to the Nordic board nRF52840 DK. The pulse signal is transmitted to the receiver, and the receiver obtains CIR data using the proposed antenna connected to the DW3000 module. For each case where the distance between the transmitter and receiver is 0.3 m, 1 m, and 2 m, the DoA information of the transmitted signal from the incident angle –30° to 30° is obtained at 5° intervals. Herein, the transmitter sends pulse signals from a fixed position, and the receiver is mounted on a rotating table to receive the signals. Fig. 11 shows the measured DoA results for the incident angle using the proposed antenna. The estimation results at the distances of 0.3 m, 1 m, and 2 m are indicated by blue, red, and green solid lines with circle markers, respectively, and the ideal DoA result is indicated by a black dashed line. The test setup is configured with the transmitter positioned at predefined

angles (e.g., −30°, −15°, 0°, 15°, 30°) relative to the receiving antenna, and these known positions are used as the reference or "Ideal DoA" values for evaluation. As a result, the root mean square (RMS) errors at measurement distances are 1.1°, 1.2°, and 1.5°, respectively. The DoA estimation results according to the incident angle are very similar to the ideal DoA results. These results demonstrate that the proposed UWB compact chip antenna can operate in mobile devices equipped with UWB direction-finding system. For comparisons, Table 2 describes key performances of the proposed antenna and previous UWB antenna studies [34], [35], [36], which includes antenna type, operating frequency range, number of radiators, aperture size, thickness, and applications. The proposed antenna has wideband characteristics from 7 GHz to 9 GHz, utilizing a single tripod-shaped radiator. It also achieves a compact design, with an aperture size of 0.7 λ and a thickness of 0.8 mm, using a high-permittivity ceramic substrate. These dimensions are notably smaller than those of conventional UWB MIMO antennas. As a result, the proposed UWB SRMP antenna is realized on a single substrate using a single tripod-shaped radiator, which can replace multiple radiators while maintaining a compact size. Although the proposed antenna features a three-port configuration, its primary design objective is direction-finding using spatially diversified CIR measurements. In particular, the three-port configuration is intended to extract CIRs for DoA estimation, rather than to improve signal diversity or channel capacity. Therefore, conventional MIMO metrics such as envelope correlation coefficient (ECC) or capacity analysis are not considered within the scope of this study. Nonetheless, we recognize that a formal MIMO diversity analysis could offer further insight into the antenna's broader applicability and will investigate ECC and capacity performance in future studies.

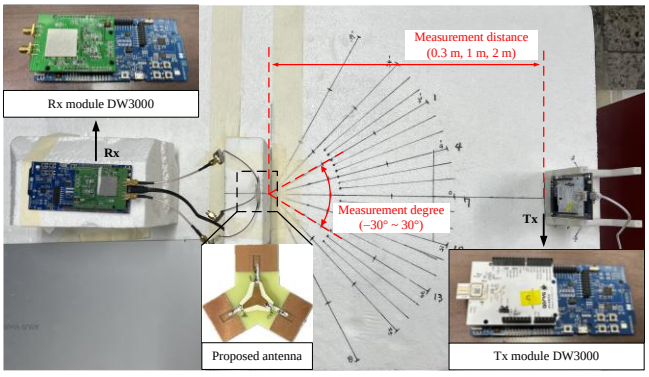

FIGURE 10. **Measurement set-up for UWB DoA estimation.**

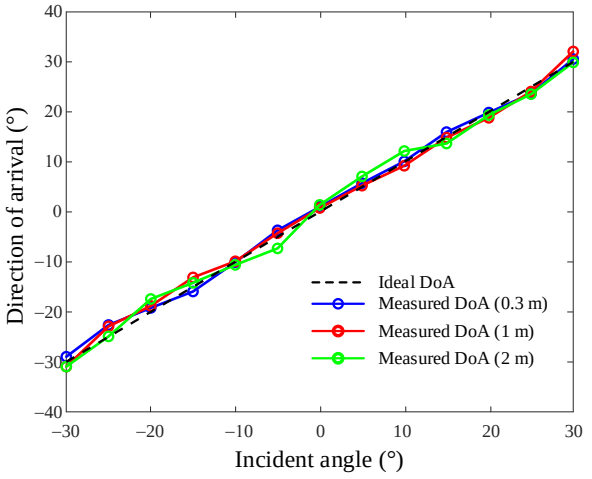

FIGURE 11. **Results of the DoA estimation using the proposed antenna.**

TABLE 2. Comparisons of performance of the proposed antenna with recent UWB MIMO antennas.

	Proposed antenna	[34]	[35]	[36]
Antenna type	**SRMP (Tripod)**	MIMO (T-shaped slot)	MIMO (Slot)	MIMO (Stub at ground)
Operating Frequency	**7–9 GHz**	3–11 GHz	3–12 GHz	3.1–10.6 GHz
Peak gain	**4.2 dBi (at 8 GHz)**	3.6 dBi (at 8 GHz)	1.9 dBi (at 8 GHz)	3.5 dBi (at 8 GHz)
The number of radiators	**1**	2	1	1
Aperture size	**0.7 λ (at 8 GHz)**	1.8 λ (at 8 GHz)	1.7 λ (at 8 GHz)	1.4 λ (at 10 GHz)
Antenna thickness	**1.6 mm**	0.8 mm	0.8 mm	1.0 mm
Application	**UWB system**	UWB system	UWB system	UWB system

IV. CONCLUSION

In this paper, we proposed a SRMP compact chip antenna for UWB direction-finding. The proposed antenna used a single tripod-shaped radiator to achieve broadband characteristics while reducing the size of an array system. To further reduce the antenna size, a high-permittivity ceramic substrate was employed. In addition, the proposed antenna mounted on the main board was designed to consider mobile devices. The compact size of MHF-7S connector was also utilized due to limited mounting space. The proposed antenna had a broadband characteristic from 7 GHz to 9 GHz for port 1. The measured mutual couplings for ports 1 and 2 had less than −12 dB across the entire operating frequency range. Also, the proposed antenna measured bore-sight gain of 4.2 dBi for port 1 at 8 GHz. To estimate the UWB direction-finding performance of the proposed antenna, the commercial Qorvo DW3000 module was used to obtain CIR data. The CIR data

was measured from the incident angle –30° to 30° with 5° intervals at distances of 0.3 m, 1 m, and 2 m. The DoA estimation results with the CIR data had RMS errors of 1.1°, 1.2°, and 1.5°. The accuracy of the estimated DoA confirms that the multi-port configuration of the proposed antenna enables effective spatial discrimination without the need for a traditional antenna array. The results demonstrated that the proposed antenna could operate in mobile devices equipped with UWB direction-finding system. This study contributes to the advancement of UWB direction-finding technology and its potential for integration into small mobile devices.

REFERENCES

[1] L. Zwirello, T. Schipper, M. Harter, and T. Zwick, "UWB localization system for indoor applications: Concept, realization and analysis," *J. Elect. Comput. Eng.*, vol. 2012, no. 1, pp. 1–12, 2012.

[2] A. R. J. Ruiz and F. S. Granja, "Comparing ubisense, bespoon, and decawave UWB location systems: Indoor performance analysis," *IEEE Trans. Instrum. Meas.*, vol. 66, no. 8, pp. 2106–2117, Aug. 2017.

[3] L. Barbieri, M. Brambilla, A. Trabattoni, S. Mervic, and M. Nicoli, "UWB localization in a smart factory: Augmentation methods and experimental assessment," *IEEE Trans. Instrum. Meas.*, vol. 70, pp. 1–18, 2021.

[4] R. J. Fontana, "Recent system applications of short-pulse ultra-wideband (UWB) technology," *IEEE Trans. Microw. Theory Tech.*, vol. 52, no. 9, pp. 2087–2104, 2004.

[5] J. Y. Siddiqui, C. Saha, and Y. M. Antar, "Compact SRR loaded UWB circular monopole antenna with frequency notch characteristics," *IEEE Trans. Antennas Propag.*, vol. 62, no. 8, pp. 4015–4020, Aug. 2014.

[6] A. M. Abdelraheem and M. A. Abdalla, "Compact curved half circular disc-monopole UWB antenna," *Int. J. Microw. Wirel. Technol.*, vol. 8, no. 2, pp. 283–290, 2016.

[7] X. L. Liang, S. S. Zhong, and W. Wang, "UWB printed circular monopole antenna," *Microw. Opt. Technol. Lett.*, vol. 48, no. 8, pp. 1532–1534, 2006.

[8] M. G. N. Alsath and M. Kanagasabai, "Compact UWB monopole antenna for automotive communications," *IEEE Trans. Antennas Propag.*, vol. 63, no. 9, pp. 4204–4208, Sep. 2015.

[9] A. Bekasiewicz and S. Koziel, "Structure and computationally efficient simulation-driven design of compact UWB monopole antenna," *IEEE Antennas Wireless Propag. Lett.*, vol. 14, pp. 1282–1258, Feb. 2015.

[10] G. Nurhayati, T. Hendrantoro, T. Fukusako, and E. Setijadi, "Mutual coupling reduction for a UWB coplanar Vivaldi array by a truncated and corrugated slot," *IEEE Antennas Wireless Propag. Lett.*, vol. 17, no. 12, pp. 2284–2288, Sep. 2018.

[11] K. Mekki, O. Necibi, S. Lakhdhar, and A. Gharsllah, "A UHF/UWB monopole antenna design process integrated in an RFID reader board," *J. Electromagn. Eng. Sci.*, vol. 22, no. 4, pp. 479–487, Jul. 2022.

[12] A. A. R. Saad and H. A. Mohamed, "Conceptual design of a compact four-element UWB MIMO slot antenna array," *IET Microw. Antennas Propag.*, vol. 13, no. 2, pp. 208–215, 2019.

[13] S. Mandal, A. Karmakar, H. Singh, S. K. Mandal, R. Mahapatra, and A. K. Mal, "A miniaturized CPW-fed on-chip UWB monopole antenna with band-notch characteristics," *Int. J. Microw. Wirel. Technol.*, vol. 12, no. 1, pp. 95–102, 2020.

[14] S. Mandal, S. K. Mandal, A. K. Mal, and R. Mahapatra, "A UWB dual band-notched on-chip antenna and its equivalent circuit model," *Prog. Electromagn. Res. B*, vol. 97, pp. 1–12, 2022.

[15] H. I. Gaha and M. Balti, "Novel bi-UWB on-chip antenna for wireless NoC," Micromachines, vol. 13, no. 2, pp. 231, 2022.

[16] J. Lee and J. K. Park, "Compact UWB chip antenna design using the coupling concept," *Prog. Electromagn. Res.*, vol. 90, pp. 341–351, 2009.

[17] W. H. Shin, S. Kibria, and M. T. Islam, "Single element MIMO antenna for LTE application with iMAT," in *Proc. IEEE Asia-Pacific Conf. Appl. Electromagn. (APACE)*, Johor Bahru, Malaysia, pp. 1–4, Dec. 2014.

[18] A. Moradikordalivand, C. Y. Leow, T. A. Rahman, and S. Ebrahimi, "Wideband MIMO antenna system with dual polarization for WiFi and LTE applications," *Int. J. Microw. Wirel. Technol.*, vol. 8, pp. 643–650, 2015.

[19] A. MoradiKordalivand, T. A. Rahman, C. Y. Leow, and S. Ebrahimi, "Dual-polarized MIMO antenna system for WiFi and LTE wireless access point applications," *Int. J. Commun. Syst.*, vol. 30, no. 8, pp. e2898, 2014.

[20] S. Chouhan, D. K. Panda, and V. S. Kushwah, "Modified circular common element four-port multiple-input-multiple-output antenna using diagonal parasitic element," *Int. J. RF Microw. Comput. Eng.*, vol. 29, no. 2, e21527, 2019.

[21] H. Nawaz and I. Tekin, "Dual port disc monopole antenna for wide-band MIMO-based wireless applications," *Microw. Opt. Technol. Lett.*, vol. 59, pp. 2942–2949, 2017.

[22] A. Chen, J. Zhang, L. Zhao, and Y. Yin, "A dual-feed MIMO antenna pair with one shared radiator and two isolated ports for fifth generation mobile communication band," *Int. J. RF Microw. Comput. Eng.*, vol. 27, no. 1, pp. e21146, 2017.

[23] A. MoradiKordalivand, T. A. Rahman, and M. Khalily, "Common elements wideband MIMO antenna system for WiFi/LTE access point applications," *IEEE Antennas Wireless Propag. Lett.*, vol. 13, pp. 1601–1604, 2014.

[24] S. R. Patre and S. P. Singh, "Shared radiator MIMO antenna for broadband applications," *IET Microw. Antennas Propag.*, vol. 12, no. 7, pp. 1153–1159, 2018.

[25] S. Youn, B. J. Jang, and H. Choo, "Design of a UWB antenna with multiple ports on a single circular radiator for direction-finding applications," *J. Electromagn. Eng. Sci.*, vol. 23, no. 1, pp. 63–68, 2023.

[26] H. Kang, S. Youn, and H. Choo, "Design of a single circular radiator with multiple patterns for a UWB three-axis monopulse system," *IEEE Access*, pp. 83887–83895, 2023.

[27] S. Youn, S. Ohm, B. J. Jang, and H. Choo, "Design of a tripod-shaped radiator patch antenna for ultra-wideband direction finding," *Sensors*, vol. 23, no. 22, pp. 9157–9169, 2023.

[28] J. Keun, S. Youn, and H. Choo, "Design of a compact direction-finding antenna using single-radiator multiple-port for UWB mobile applications," *IEEE Access*, pp. 138610–138616, 2024.

[29] FEKO EM Software. Altair. [Online]. Available: https://www.altair.co.kr/feko/. Accessed: Jun. 1, 2024.

[30] L. Malviya and S. Chouhan, "Multi-cut four-port shared radiator with stepped ground and diversity effects for WLAN application," *Int. J. Microw. Wirel. Technol.*, vol. 11, pp. 1044–1053, 2019.

[31] H. T. Chattha, M. Nasir, Q. H. Abbasi, Y. Huang, and S. S. AlJa'Afreh, "Compact low-profile dual-port single wideband planar inverted-F MIMO antenna," *IEEE Antennas Wirel. Propag. Lett.*, vol. 12, pp. 1673–1675, 2013.

[32] G. Srivastava and B. K. Kanaujia, "Compact dual band-notched UWB MIMO antenna with shared radiator," *Microw. Opt. Technol. Lett.*, vol. 57, pp. 2886–2891, 2015.

[33] C. A. Balanis, *Antenna Theory: Analysis and Design*, 4th ed. Hoboken, NJ, USA: Wiley, 2016

[34] C.-X. Mao and Q.-X. Chu, "Compact coradiator UWB-MIMO antenna with dual polarization," *IEEE Trans. Antennas Propag.*, vol. 62, no. 9, pp. 4474–4480, Sep. 2014.

[35] G. Srivastava, B. K. Kanaujia, and R. Paulus, "UWB MIMO antenna with common radiator," *Int. J. Microw. Wireless Technol.*, vol. 9, no. 3, pp. 573–580, Mar. 2017.

[36] J.-Y. Zhang, F. Zhang, and W.-P. Tian, "Compact 4-port ACS-fed UWB-MIMO antenna with shared radiators," *Prog. Electromagn. Res. Lett.*, vol. 55, pp. 81–88, 2015.

HYUNMU KANG received the B.S. and M.S. degree in electronic and electrical engineering from Hongik University, Seoul, South Korea, in 2023 and 2025, respectively. He is currently a Research Engineer with LIG Nex1 Company, South Korea. His main research interests include SAR antennas, satellite systems, UWB antennas, direction-finding.

HOSUNG CHOO (S'00–M'04–SM'11) received the B.S. degree in radio science and engineering from Hanyang University, Seoul, South Korea, in 1998, and the M.S. and Ph.D. degrees in electrical and computer engineering from the University of Texas at Austin, in 2000 and 2003, respectively. In September 2003, he joined the School of Electronic and Electrical Engineering, Hongik University, Seoul, where he is currently a professor. His principal areas of research include electrically small antennas for wireless communications, reader and tag antenna for RFID, on-glass and conformal antennas for vehicles and aircraft, and array antenna for GPS applications.

SANGWOON YOUN received the B.S., M.S., and Ph.D degrees in electronic and electrical engineering from Hongik University, Seoul, South Korea, in 2019, 2021, and 2024, respectively. In September 2024, he was a Postdoctoral Researcher in Hongik Univesity. He is currently an assistant professor with the Department of Digital Information and Communication Technology Engineering, Gyeongkuk National University. His research interests include EMI and EMC, wave propagation, UWB antennas, 5G application, direction-finding, and satellite communication systems.